



LGR6 marks nephron progenitor cells

Ravian L. van Ineveld^{1,2} | Thanasis Margaritis¹  | Berend A.P. Kooiman¹ |
 Femke Groenveld³ | Hendrikus C.R. Ariese^{1,2} | Philip Lijnzaad¹ |
 Hannah R. Johnson^{1,2} | Jeroen Korving³ | Ellen J. Wehrens^{1,2} |
 Frank Holstege¹ | Jacco van Rheenen^{2,4} | Jarno Drost^{1,2} | Anne C. Rios^{1,2} |
 Frank L. Bos^{1,2} 

¹Princess Máxima Center for Pediatric Oncology, Utrecht, The Netherlands

²Oncode Institute, Utrecht, The Netherlands

³Hubrecht Institute, Royal Netherlands Academy of Arts and Sciences (KNAW) and University Medical Center (UMC) Utrecht, Utrecht, The Netherlands

⁴Division of Molecular Pathology, The Netherlands Cancer Institute, Amsterdam, The Netherlands

Correspondence

Frank L. Bos, Princess Máxima Center for Pediatric Oncology
 Utrecht, The Netherlands.
 Email: f.l.bos-3@prinsesmaximacentrum.nl

Funding information

Cancer Genomics Centre; European Research Council, Grant/Award Number: 648804; European Research Council advanced, Grant/Award Number: 671174; European Research Council starting grant, Grant/Award Number: 804412; KWF Kankerbestrijding, Grant/Award Number: 6660

Abstract

Background: Nephron progenitor cells (NPCs) undergo a stepwise process to generate all mature nephron structures. Mesenchymal to epithelial transition (MET) is considered a multistep process of NPC differentiation to ensure progressive establishment of new nephrons. However, despite this important role, to date, no marker for NPCs undergoing MET in the nephron exists.

Results: Here, we identify LGR6 as a NPC marker, expressed in very early cap mesenchyme, pre-tubular aggregates, renal vesicles, and in segments of S-shaped bodies, following the trajectory of MET. By using a lineage tracing approach in embryonic explants in combination with confocal imaging and single-cell RNA sequencing, we provide evidence for the multiple fates of LGR6+ cells during embryonic nephrogenesis. Moreover, by using long-term in vivo lineage tracing, we show that postnatal LGR6+ cells are capable of generating the multiple lineages of the nephrons.

Conclusions: Given the profound early mesenchymal expression and MET signature of LGR6+ cells, together with the lineage tracing of mesenchymal LGR6+ cells, we conclude that LGR6+ cells contribute to all nephrogenic segments by undergoing MET. LGR6+ cells can therefore be considered an early committed NPC population during embryonic and postnatal nephrogenesis with potential regenerative capability.

KEYWORDS

3D imaging, fate, LGR6, lineage tracing, mesenchymal to epithelial transition, nephron progenitor cells

Ravian L. van Ineveld and Thanasis Margaritis equally shared first authorship.

Anne C. Rios and Frank L. Bos equally shared senior authorship.

1 | INTRODUCTION

Nephron progenitor cells (NPCs) are found in cap mesenchyme (CM) of the developing kidney and undergo a

This is an open access article under the terms of the Creative Commons Attribution-NonCommercial-NoDerivs License, which permits use and distribution in any medium, provided the original work is properly cited, the use is non-commercial and no modifications or adaptations are made.

© 2021 The Authors. *Developmental Dynamics* published by Wiley Periodicals LLC on behalf of American Association of Anatomists.

stepwise process to generate mature nephron structures.¹ Nephrogenesis starts when WNT9B secreted by the ureteric buds (UBs) activates canonical B-catenin in NPCs.² Next, WNT4 triggers mesenchymal to epithelial transition (MET), causing NPCs to accumulate into pre-tubular aggregates (PTA) that will become renal vesicles (RVs).²⁻⁶ The RV develops further and patterns along the proximal-distal axis, which ultimately leads to the formation of an s-shaped body (SSB) that gives rise to nephron segments.⁷ Extensive lineage tracing studies *in vivo* and in kidney explants have shown that, by labeling single CM cells, both SIX2+ and CITED1+ CM cells can be multipotent, self-renewing kidney stem cells.^{3,8}

Leucine rich repeat containing G protein coupled receptors (Lgrs) are of considerable interest, as they mark stem cell in various tissues.⁹ The LGR5-GFP-IRES-creERT2 model demonstrated the expression of LGR5-GFP+ cells in the renal cortex around embryonic day (E)14, coinciding with the onset of nephrogenesis and lineage tracing studies revealed that these cells can contribute to certain nephrogenic structures, including the thick ascending loop of Henle, the distal convoluted tubule, and the connecting segment of the nephron.¹⁰ Moreover, within the embryonic kidney, LGR4 and LGR5 expression are co-expressed in tubular epithelium and not present in early CM. Functional studies have revealed that Lgr4-deficient mice showed dilated tubules and cyst formation, whereas Lgr5 deletion did not lead to any kidney defects.^{11,12} Thus, available data indicate that LGR4 and LGR5 do not mark early progenitors in CM and cannot drive differentiation of all nephrogenic structures.

Another Lgr, LGR6, has been shown to mark stem cells in various organs, including lung, nail, skin, taste bud, and mammary gland,^{9,13-15} yet its implication in nephrogenesis remains undefined. Here, we set out to investigate whether LGR6 is implicated in early nephrogenesis by analyzing the expression and fate of LGR6+ cells in the developing kidney. We report expression of LGR6 during embryonic and postnatal nephrogenesis and importantly provide evidence that LGR6+ cells are NPCs that can contribute to multiple nephrogenic cell types during both embryonic and postnatal kidney development.

2 | RESULTS

2.1 | Mesenchymal LGR6 marks early nephron progenitor populations during nephrogenesis

To unravel the expression of LGR6 during embryonic kidney development, we made use of LGR6 reporter mice (LGR6-EGFP-IRES-CreERT2), in which LGR6 expressing

cells are marked by green fluorescent protein (GFP).¹³ We characterized LGR6-GFP+ cells in the developing kidney at E11.5, E12.5, and E13.5, by co-staining thick vibratome sections with CM marker SIX2, epithelial marker CDH1 and anti-GFP (Figure 1A). At E11.5, LGR6-GFP expressing cells were found in SIX2+ CM surrounding UBs (Figure 1B). At E12.5 and E13.5, LGR6-GFP+ cells were also found in PTA, RV and SSB structures, directly correlating LGR6 expression with nephrogenic MET stages and thus the onset of nephrogenesis (Figure 1C-E, Movie S1). This was further strengthened by comparing expression levels of SIX2 within LGR6-GFP+ cells between early nephrogenic developmental timepoints. At E11.5, LGR6-GFP+ cells expressed the highest levels of SIX2 whereas, a reduction in SIX2, coinciding with the onset of nephrogenesis,¹⁶ was observed in E13.5 LGR6-GFP+ cells (Figure 1F). We next quantified the expression of LGR6-GFP and SIX2 in entire developing kidneys to reveal and compare the relative expression of SIX2 and LGR6-GFP per nephrogenic stage (CM, PTA/RV, and SSB) using Large-scale Single-cell Resolution 3D (LSR-3D) imaging¹⁷ (Figure 1G, Movie S2). Single cell segmentation of 1241 cells revealed expression of LGR6-GFP in CM, PTA/RV, and SSB, thereby marking all nephrogenic compartments at E13.5. This also demonstrated that SSB's have fewer GFP+ cells compared with CM and PTA/RV and revealed a reduction in SIX2 expression along the differentiating structures toward epithelium, in accordance with MET (Figure 1H). Together, these results show that between E11.5 and E13.5, LGR6 is expressed by mesenchymal cells in CM, cells undergoing MET in the PTA/RV and committed cells in SSB, which would match with a NPC identity.

Since we observed expression of LGR6 as early as E11.5 (Figure 1B), coinciding with the start of nephrogenesis and MET, we aimed to characterize the RNA signatures of these first LGR6-GFP+ expressing cells in the developing kidney by performing single-cell RNA sequencing (scRNAseq). Cells (GFP+ and GFP-) from E11.5 kidneys clustered into 10 populations; (1) macrophages, (2) angioblasts, (3-6) stromal cells, (7) cells of the CM, (8) committed NPCs, (9) cells belonging to PTA/RVs, and (10) epithelial cells (Figure 2A,C). The top 50 genes expressed by each cluster and GO analysis confirmed known markers and functions of each cell population (data not shown). Accordingly, we identified cluster 7-9 to be nephrogenic populations (Figure 2D). LGR6-GFP+ sorted cells were enriched in the nephrogenic population as a whole ($P = .00001$) (Figure 2B,C), as well as within the committed NPC population ($P = .03$) and PTA/RV population ($P = .0014$). This shows that LGR6 expressing cells are nephrogenic, belonging to NPCs and undergoing MET. By analyzing

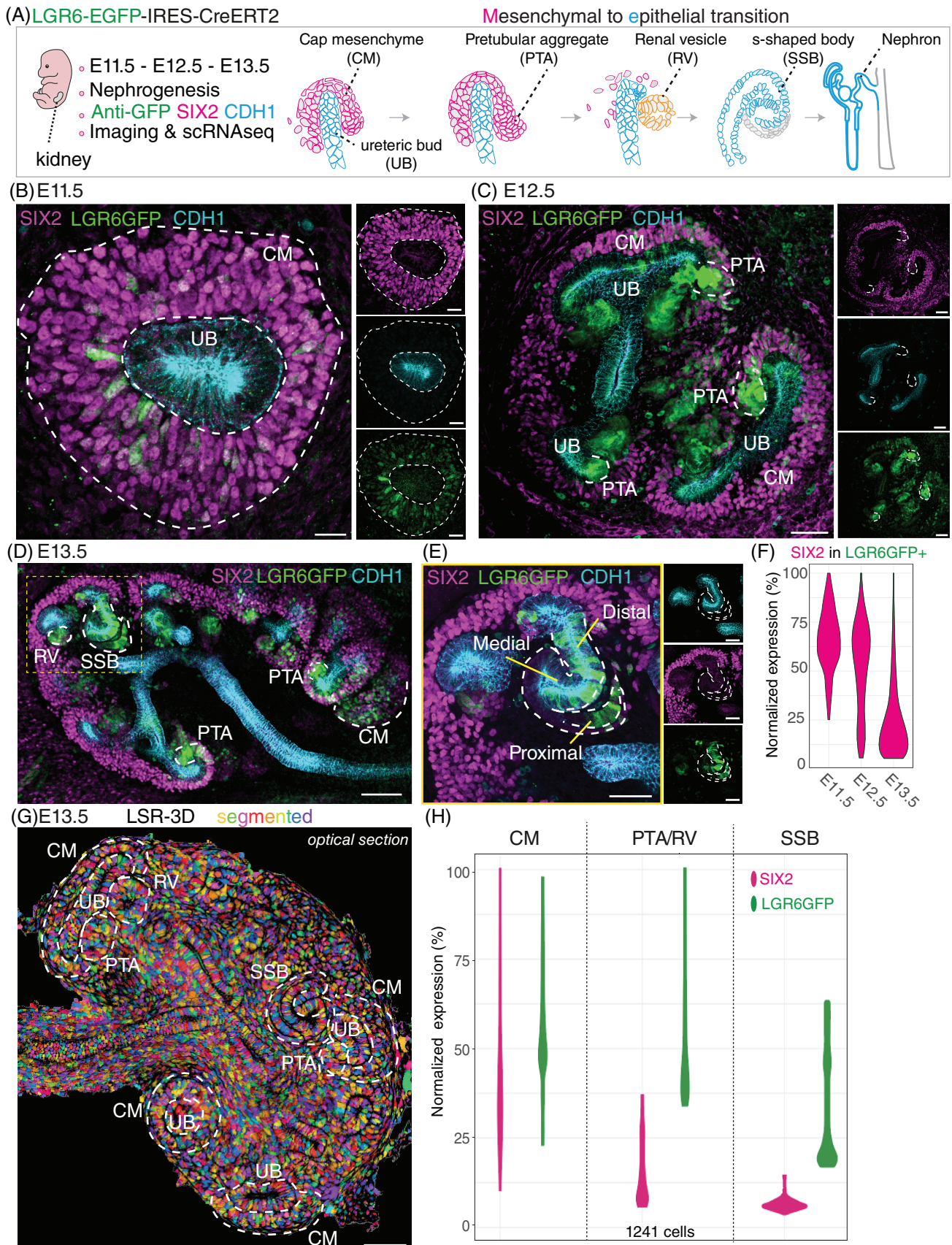


FIGURE 1 Legend on next page.

expression of key nephrogenic MET marker genes, we were able to reveal elevated expression of *Jag1*, *Wnt4*, and *Pax8* in the PTA/RV population (Figure 2E) and elevated levels of *Sall1* and a reduction of *Six2* in PTA/RV (Figure 2F).

To investigate if the observed specificity of LGR6 for NPCs undergoing MET extends to human nephrogenesis, we used a recently published human embryonic kidney scRNA-seq dataset.¹⁸ The data reveals LGR6 expression in cap mesenchyme, peaking at proliferating cap mesenchyme, and in the derived RV, but absent in UB or further differentiated nephron cells (Figure 2G). Thus, our imaging and scRNAseq data show that LGR6-GFP⁺ cells reside within nephrogenic compartments and harbor an NPC and MET signature, as early as E11.5 in mice and possibly during human development as well.

2.2 | Lineage tracing of LGR6⁺ cells confirms a nephrogenic fate

To investigate the fate of LGR6-GFP⁺ cells and their subsequent contribution to nephrogenesis, we crossed LGR6-EGFP-IRES-CreERT2 mice to ROSA26-tdTomato reporter mice to induce a permanent mark upon LGR6 expression and individually monitored marked cells in kidney explants (Figure 3A). A brief induction with 4-hydroxytamoxifen (1 hour) in E11.5 and E12.5 explants ensured recombination, allowing to reliably track individual cells. Traced cells could be monitored for long periods of time, up to 7 days (Figure 3A,B). From 24 hours after induction to 168 hours after onset of explant culture, we observed clonal expansion of tdTom⁺ cells within in CM, PTAs, RVs, comma-shaped bodies (CSBs), and SSBs (Figure 3B,C, Movie S2), revealing the cellular fate of LGR6 expressing cells over time. After 168 hours, LGR6⁺ cells are NPCs and are able to commit to nephrogenesis and epithelization, as confirmed by tdTom⁺ cells expressing NPC marker SIX2 (Figure 3D, yellow arrowheads) and epithelial marker CDH1

(Figure 3D, white arrowheads), respectively (Movie S2). We further delineated the fate of early, E11.5 and E12.5, LGR6⁺ cells by performing scRNAseq analysis on sorted tdTom⁺ and tdTom⁻ cells after long term explant culture (Figure 4A-C). Cells clustered into six populations; (1) macrophages, (2) endothelial cells, (3-5) stromal, and (6) nephrogenic cells with tdTom⁺ cells significantly enriched in the nephrogenic population (adj *P*-val = 2.1×10^{-20}) (Figure 4D), revealing the subsequent predominantly nephrogenic fate of early LGR6⁺ cells. Furthermore, we used a marker-based approach to further subset the nephrogenic tdTom transcript positive cells. This revealed multiple fates of early LGR6⁺ cells, with individual cells displaying a nephrogenic epithelial fate (*Epcam*), a mesenchymal/NPC fate (*Sall1*, *Six2*, and *Cited1*) and a MET transitioning fate (*Wnt4*, *Pax8*, *Jag1*, and *Lhx1*) (Figure 4E). Strikingly, our analysis also revealed that cells with tdTom transcripts expressed proximal SSB and podocyte progenitor markers (*Wt1*, *Mafb*, *Podxl*, and *Ptpro*; Figure 4E), indicating that early LGR6-GFP⁺ cells can follow a podocyte lineage as well. This marker-based lineage commitment of the LGR6-GFP⁺ cells was further corroborated using the -above-mentioned independent human embryonic kidney dataset¹⁸ by scoring the individual cells based on the top 20 markers of the mesenchyme progenitors (cap mesenchyme), podocyte lineage (podocytes), and epithelial nephron lineage (distal SSB) (Figure 4F,G). The results of this analysis are in line with the established mouse marker-based approach used above. Together, these results show that early mesenchymal LGR6-GFP⁺ are giving rise to mesenchymal, epithelial and podocyte lineages, revealing multiple fates of LGR6⁺ cells.

2.3 | Postnatal LGR6⁺ cells contribute to multiple specifics of the adult nephron

Having established the nephrogenic fate of embryonic LGR6 expressing cells, we next aimed to elucidate the

FIGURE 1 The 3D Imaging of LGR6-GFP⁺ cells reveal a MET and NPC identity during embryonic nephrogenesis. (A) Graphical representation of experimental setup of Figures 1 and 2 and the different MET-driven stages of nephron development. (B) Representative vibratome section of E11.5 LGR6-EGFP-IRES-CreERT2 mouse kidney stained with anti-SIX2 (magenta), anti-CDH1 (cyan), and anti-GFP (green). Scale bar 20 μ m. (C) Representative vibratome section of E12.5 LGR6-EGFP-IRES-CreERT2 mouse kidney stained with anti-SIX2 (magenta), anti-CDH1 (cyan), and anti-GFP (green). Scale bar 50 μ m. (D) Representative vibratome section of E13.5 LGR6-EGFP-IRES-CreERT2 mouse kidney stained with anti-SIX2 (magenta), anti-CDH1 (cyan) and anti-GFP (green). Scale bar 100 μ m. (E) Magnified area indicated in Figure D. Dashed white lines surround the SSB. Scale bar 50 μ m. (F) Single cell quantification of normalized expression levels of SIX2 in LGR6⁺ segmented cells at E11.5, E12.5 and E13.5. (G) Representative image of single-cell segmented LSR-3D imaged E13.5 whole mount kidneys (n = 2). (H) Single-cell quantification of normalized LGR6-GFP⁺ (green) and SIX2 (magenta) expression in representative region of interest, in a total of 1241 cells divided over the different nephrogenic structures: CM, PTA/RV, and SSB. Scale bar 100 μ m. UB, ureteric bud; CM, cap mesenchyme; SSB, s-shaped body; PTA, pretubular aggregate; RV, renal vesicle

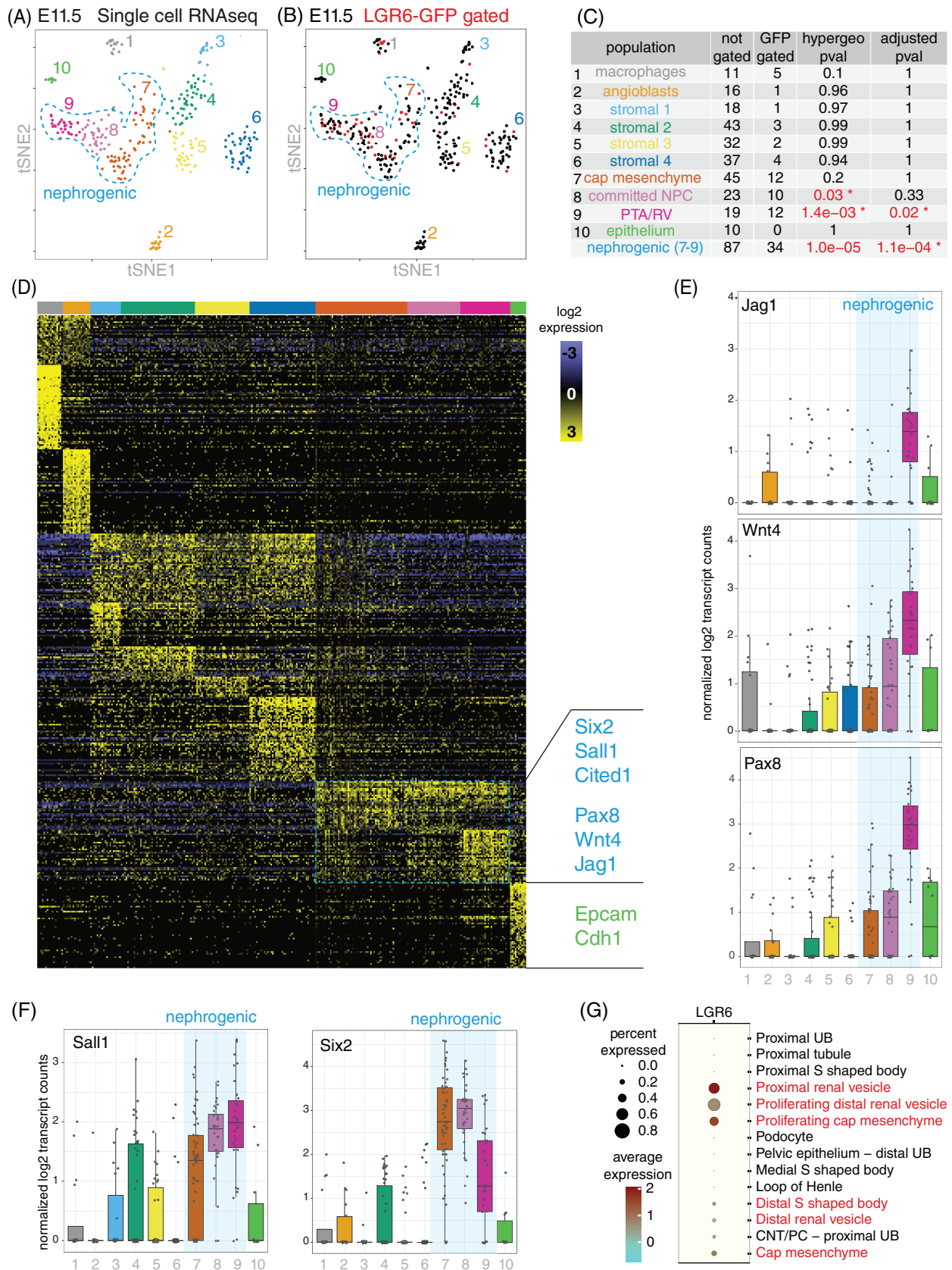


FIGURE 2 Legend on next page.

fate of LGR6⁺ cells during postnatal kidney development. Since CM and NPCs can still be found postnatally,^{19,20} we hypothesized that LGR6-GFP⁺ cells could also be present and contribute to nephrogenesis after birth and could thereby give rise to all nephrogenic segments of the adult kidney. To test this, kidneys of LGR6-EGFP-IRES-CreERT2 pups at postnatal day 1 (P1) were analyzed for GFP expression. Indeed, LGR6-GFP⁺ cells were only found in the cortex in CM, PTA, and RV, in line with nascent nephrogenesis (Figure 5A,B). These results indicate that LGR6⁺ expression is not only expressed in embryonic stages, but also during the ongoing nephrogenic wave postnatally. These LGR6⁺ cells might therefore also contribute to nephrogenesis after birth. To investigate this, lineage tracing was induced in LGR6-EGFP-IRES-CreERT2/ROSA26-tdTomato pups at P1 and tdTom⁺ cells were analyzed at P3. At P3, LSR-3D imaging was performed on thick vibratome sections, including markers for F-Actin and DAPI, to reveal localization and identity of traced cells.²¹ TdTom⁺ cells were exclusively found in the cortex within the nephrogenic zone, indicative of nascent nephrogenesis (Figure 5C). In addition, by staining for JAG1, WT1, and CDH1 we were able to further delineate this exclusive distribution within nephrogenic compartments; all tdTom⁺ cells were restricted to PTA, RV, and CSBs, as well as distal, medial and proximal parts of SSBs, coinciding with newly developing epithelial structures surrounding CDH1⁺ UB (Figure 5D-F). Finding tdTom⁺ cells exclusively in these structures at P3 hints toward a multipotent nephrogenic fate of LGR6⁺ cells at P1 to adulthood.

To provide further evidence for potency of LGR6⁺ cells postnatally, we traced LGR6-GFP⁺ cells from P1 throughout the postnatal stages (P7 and P14), puberty (P36), and adulthood (P77) (Movie S3). At P7, tdTom⁺ clones were evident in the outer cortex only, corresponding with nascent nephrogenesis (Figure 5G). Based on F-Actin and DAPI staining, tdTom⁺ clones in the distal tube (DT), proximal tube (PT), and glomerulus (GL) of the nephron could already be identified

(Figure 5H, left panel). To confirm that these clones within the cortex were of epithelial identity, we also stained sections with CDH1 and revealed CDH1⁺ clones, thus considered to be epithelial (Figure 5H, right panel, red arrows). In addition, clones within the GL expressed WT1 and appeared to have a podocyte-like morphology (Figure 5H, right panel, yellow arrows). The ongoing contribution to nephron segments and podocytes was further strengthened at P14, which revealed tdTom⁺ clones in the cortex as well, within clearly identifiable DT, PT, and GL and even podocytes of the glomerulus (Figure 5I). If LGR6 expression is restricted to nephrogenesis, we would expect little to no contribution to nephrogenesis of cells in which LGR6 tracing is induced beyond the nephrogenic phase, after P4.²⁰ Indeed, when LGR6 tracing was induced in P7 pups and cells were traced for 1 week, they did not reveal any nephrogenic contribution at P14 (Figure 5J) and very limited tdTom⁺ cells were found back (yellow arrows), coinciding with the last wave of nephrogenesis in mice. Taken together, based on the observation that traced P1 LGR6⁺ cells are found at P3 in all nephrogenic compartments and give rise to specialized epithelial structures at P7 and P14, we conclude that postnatal LGR6⁺ cells are nephrogenic and can give rise to epithelial tubes and cells of the glomerulus, such as podocytes.

Lastly, to reveal the long-term permanent contribution of LGR6⁺ cells to nephrogenesis, we analyzed P1 induced traced kidneys at P36 (Figure 6A), P77 (Figure 6B), and P150 (data not shown) and found long ribbons of tdTom⁺ cells spanning the entire cortex length and into the medulla, looping back to the cortex, indicative of the ascending and descending parts of the Loop of Henle (LOH) (Figure 6C, Movie S3). To further define the identity of the various types of nephron segments, we also used a marker-based approach. We found tdTom⁺CALBINDIN⁺ cells, showing that LGR6⁺ cells can also give rise to connecting tubules (CT) and distal convoluted tubules (DCT) as well as tdTom⁺UMOD⁺ to confirm the expression in LOH (Figure 6D). Moreover, tdTom⁺ ribbons were devoid of collecting duct

FIGURE 2 Single-cell RNA-Seq analyses of LGR6-GFP⁺ cells reveal a MET and NPC identity during embryonic nephrogenesis. (A) t-SNE plot of E11.5 embryonic kidney cells labeled according to the population ID. Dashed blue line indicates nephrogenic populations. (B) As in A, with differential labeling for non-gated cells (black) or GFP⁺ cells (red). Dashed blue line indicates nephrogenic populations. (C) Table showing absolute numbers of sorted GFP⁺ cells (GFP gated) and non-sorted (not gated) for the different embryonic kidney cell populations. Both uncorrected and the Bonferroni multiple testing corrected *P*-values of the hypergeometric test are depicted. (D) Heatmap of log₂ expression changes over the median per gene per cell population with differentially expressed genes specific for the nephrogenic (blue) and epithelial (green) populations. (E) Normalized log₂ expression of *Jag1*, *Wnt4*, and *Pax8* plotted per population ID. (F) Normalized Log₂ expression of CM/NPC markers *Sall1* and *Six2* plotted per population ID. (G) Dot plot of LGR6 expression levels among different human embryonic kidney cell types. The dot size represents the percentage of the cells of a given cell type expressing LGR6, while the color depicts the logged averaged gene expression per cell type

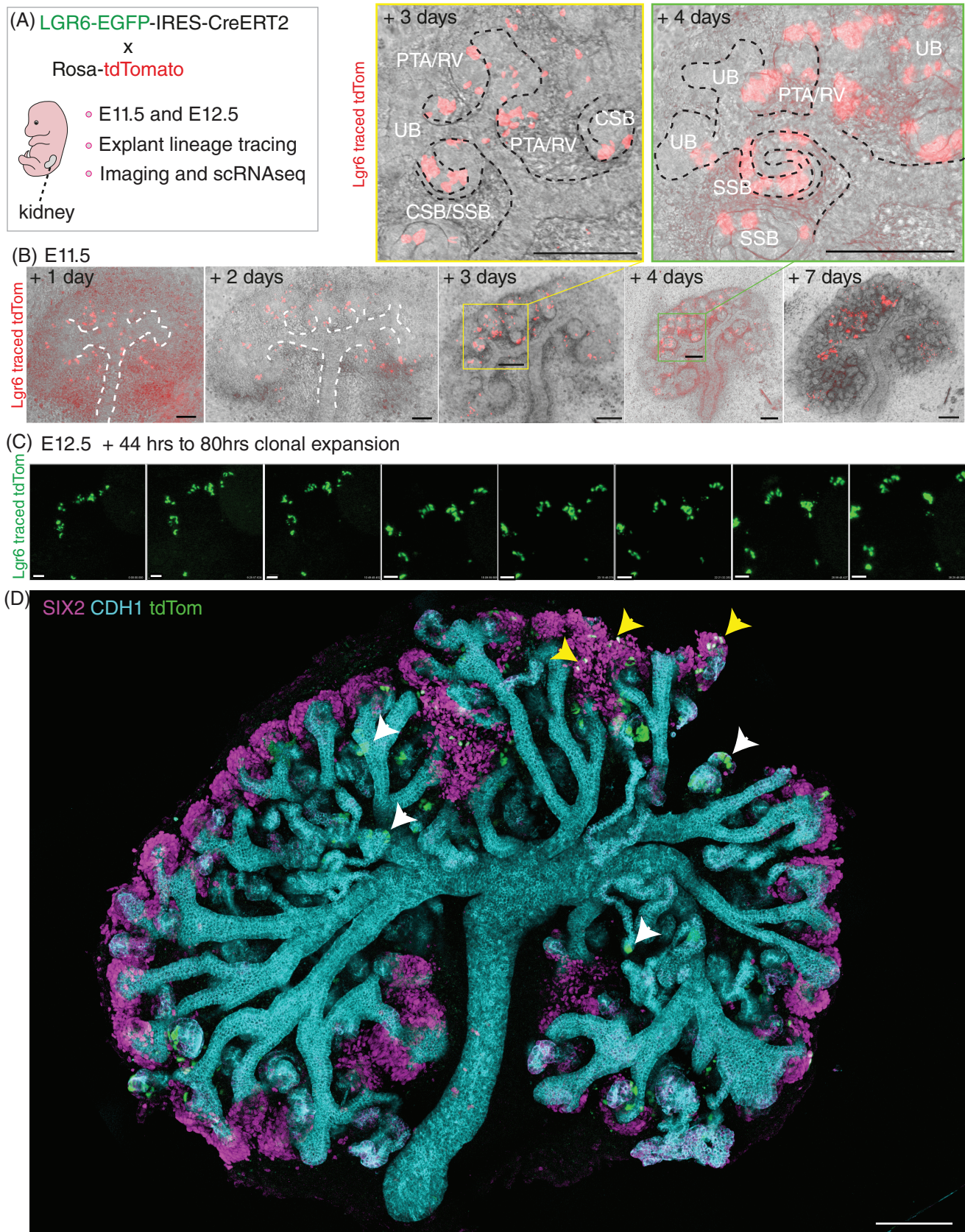


FIGURE 3 Ex vivo lineage tracing and 3D imaging of tdTom^+ cells reveal multiple fates of Lgr6^+ cells. (A) Graphical representation of experimental setup of Figures 3 and 4. (B) E11.5 **LGR6-EGFP-IRES-CreERT2 / ROSA26-tdTomato** kidney explants cultured for 7 days after tamoxifen induced lineage tracing. tdTom^+ cells in red. UB, ureteric bud; CSB, comma-shaped body; SSB, s-shaped body; PTA, pretubular aggregate; RV, renal vesicle. Scale bar 100 μm . (C) Time-lapse of E12.5 **LGR6-EGFP-IRES-CreERT2/ROSA26-tdTomato** kidney explants. tdTom^+ in green. Scale bar 50 μm . (D) E11.5 **LGR6-EGFP-IRES-CreERT2/ROSA26-tdTomato** embryonic explant cultured for 7 days after tamoxifen induction and stained with anti-SIX2 (magenta) and anti-CDH1 (cyan). tdTom^+ cells in green. Yellow arrowheads indicate $\text{SIX2}^+ \text{tdTom}^+$ cells, white arrowheads $\text{CDH1}^+ \text{tdTom}^+$ cells. Scale bar 150 μm

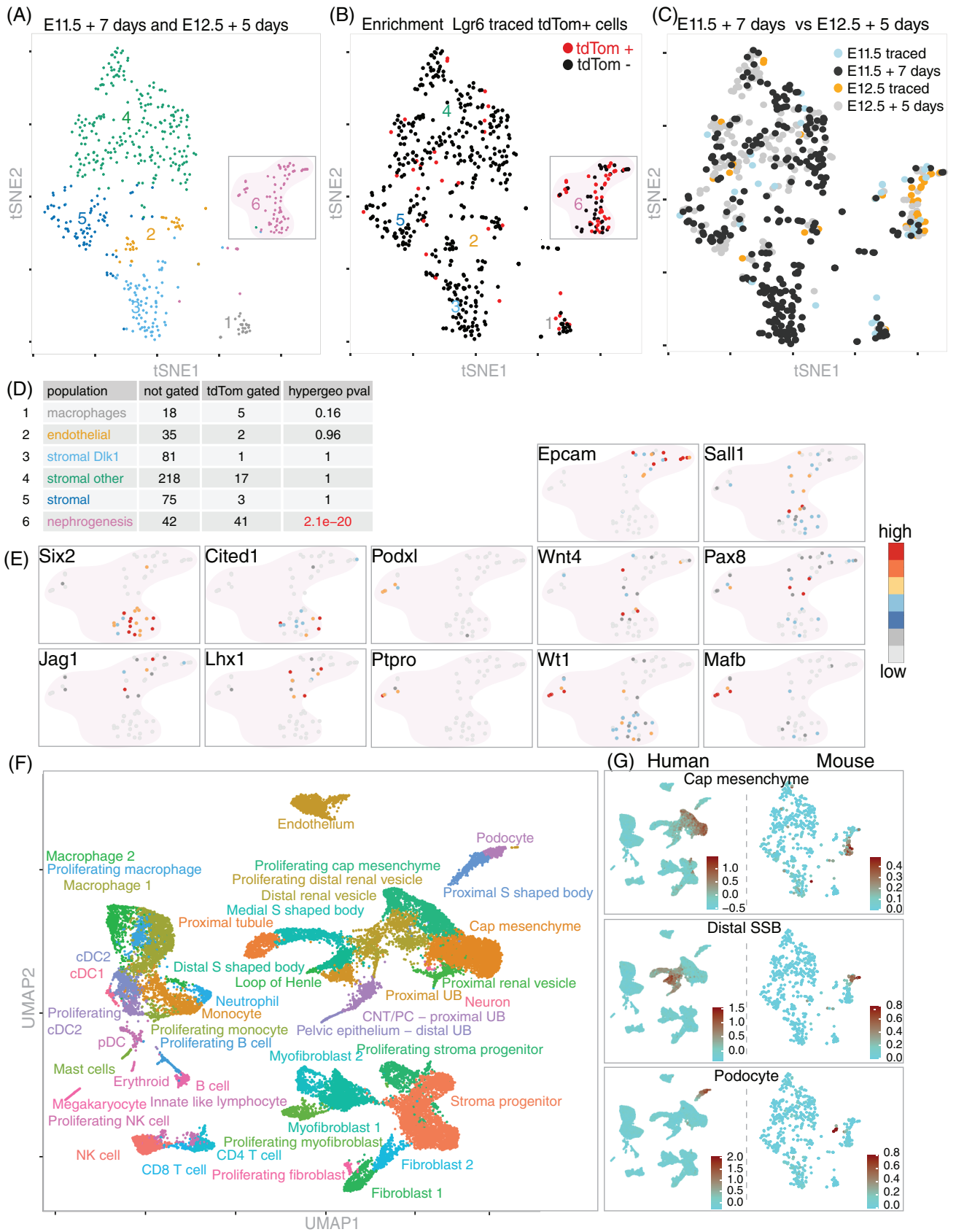


FIGURE 4 Legend on next page.

(CD) marker AQP4 (Figure 6E), showing that LGR6⁺ cells solely give rise to mesenchymal derived nephron segments and not UB derived epithelial structures.

Together, these findings show that LGR6⁺ cells contribute to embryonic nephrogenesis and continue to do so postnatally, generating cells of all mesenchymal derived segments of the nephron: LOH, CT, DCT, DT, PT, and GL (Figure 6F). Given the profound early mesenchymal expression and MET signature of LGR6⁺ cells, together with the lineage tracing of mesenchymal LGR6⁺ cells, we conclude that LGR6⁺ cells contribute to multiple nephrogenic segments by undergoing MET and can therefore be considered a true nephron progenitor cell population.

3 | DISCUSSION

Combining lineage tracing with imaging, flow cytometry, and scRNAseq, we provide evidence that at the onset and throughout kidney development, LGR6-GFP⁺ marks nephrogenic cells that are potent in generating multiple different segments of the nephron. We here found that LGR6 is expressed very early in the developing kidney, already at E11.5 and throughout embryonic and postnatal development. Expression follows the trajectory of MET and is observed in early CM, PTA, RV, CSB, and SSB. Importantly, early LGR6 expressing cells can form nephron cell lineages present in the mature kidney, indicating that LGR6 marks nephron progenitor cells.

Previously, it was shown that nephron progenitors reside within SIX2 expressing CM cells.³ Imaging of LGR6-GFP reveals that not all SIX2⁺ cells express LGR6. Considering the function of LGR6 as a regulator of the Wnt signaling pathway, a well-established pathway involved in regulating the fate of adult stem cells, we propose that LGR6 marks a subset of SIX2 CM cells with nephrogenic fate. This is corroborated by both our imaging and single cell scRNAseq data showing that LGR6 expressing cells can develop into tubular epithelium and podocytes. Thus, LGR6 positive CM cells could be more receptive to Wnt inducing signals than LGR6 negative

CM cells, determining their subsequent lineage formation. However, despite the established function of LGR6 as a regulator of the Wnt signaling pathway, LGR6 knock-out mice are viable and reported to develop normally,¹³ suggesting that LGR6 is dispensable for normal kidney development. This may imply that LGR6 merely marks stem cells without playing a direct role in nephrogenesis or that redundant regulatory pathways exist, like combined expression of WNT4.²² However, a compensatory mechanism might also occur in full knock-out mice, due to the complete lack of LGR6 expression. Compared with its direct family members LGR4 and LGR5, our data shows that LGR6 specifically marks early NPCs that can still adapt a broad nephrogenic fate. LGR6 is only expressed in early nephrogenic structures (from CM to SSB (Figure 1) and contributes to the entire nephron, whereas LGR4 and LGR5 are known to be expressed at late stages (from the RV stage onward) and only contribute to parts of the nephron.¹⁰

Up till now, identification of NPCs has been dependent on a combination of markers, some of them expressed intracellularly, hampering the isolation of NPCs for experimental or therapeutic purposes. Indeed, lineage tracing studies in mice have revealed that NPCs can be identified based on the expression of transcription factors SIX2, WT1, and CITED1, thus isolation of NPCs via single membrane marker has not been possible. Similarly, in human, a combination of two markers: the neuronal cell surface protein NCAM1 together with CD133 is required to mark SIX2⁺ multipotent renal stem cells.^{23,24} Therefore, our work, identifying LGR6, a leucine-rich G protein-coupled cell surface receptor, as a marker for NPCs opens up new avenues for therapeutic targeting and/or isolating NPCs for regeneration studies. It will therefore be useful to further investigate the conserved expression of LGR6 and if LGR6⁺ cells maintain their potential ex vivo, acting autonomously as NPCs without direct neighboring UB signals.

In sum, we here provide evidence that LGR6 marks NPCs with multiple fates and nephrogenic potential throughout kidney development, which can have important consequences for kidney regeneration attempts.

FIGURE 4 Ex vivo lineage tracing and single-cell RNA-Seq analyses of tdTom⁺ cells reveal multiple fates of Lgr6⁺ cells. (A) t-SNE plot of embryonic kidney cells from E11.5 and E12.5 explanted kidneys cultured for 7 and 5 days, respectively. Cells are labeled according to their population ID. (B) Representation of FACS sorted TdTom⁺ cells (red) within the t-SNEs of (A). (C) t-SNE plot of explanted embryonic kidney cells labeled according to the time point E11.5 + 7 days (black/blue) and E12.5 + 5 days (grey/orange). (D) Table depicting absolute numbers of tdTom positivity (tdTom gated) or not (not gated) and the Bonferroni multiple testing corrected *P*-values of the hypergeometric test. (E) t-SNE feature plots of the tdTom⁺ cells belonging to the nephrogenic cluster labeled for the expression of *Epcam*, *Sall1*, *Six2*, *Cited1*, *Podxl*, *Wnt4*, *Pax8*, *Jag1*, *Lhx1*, *Ptpro*, *Wt1*, and *Mafb*. (F) UMAP plot of human embryonic kidney dataset adapted from Figure 1E of the article Stewart et al 2019.¹⁸ (G) Lineage scoring based on modules of the top 20 markers of the annotated human fetal kidney cell types (cap mesenchyme, distal SSB, and podocyte) on the original human dataset (left panels) and our ex vivo tracing dataset (right panels)

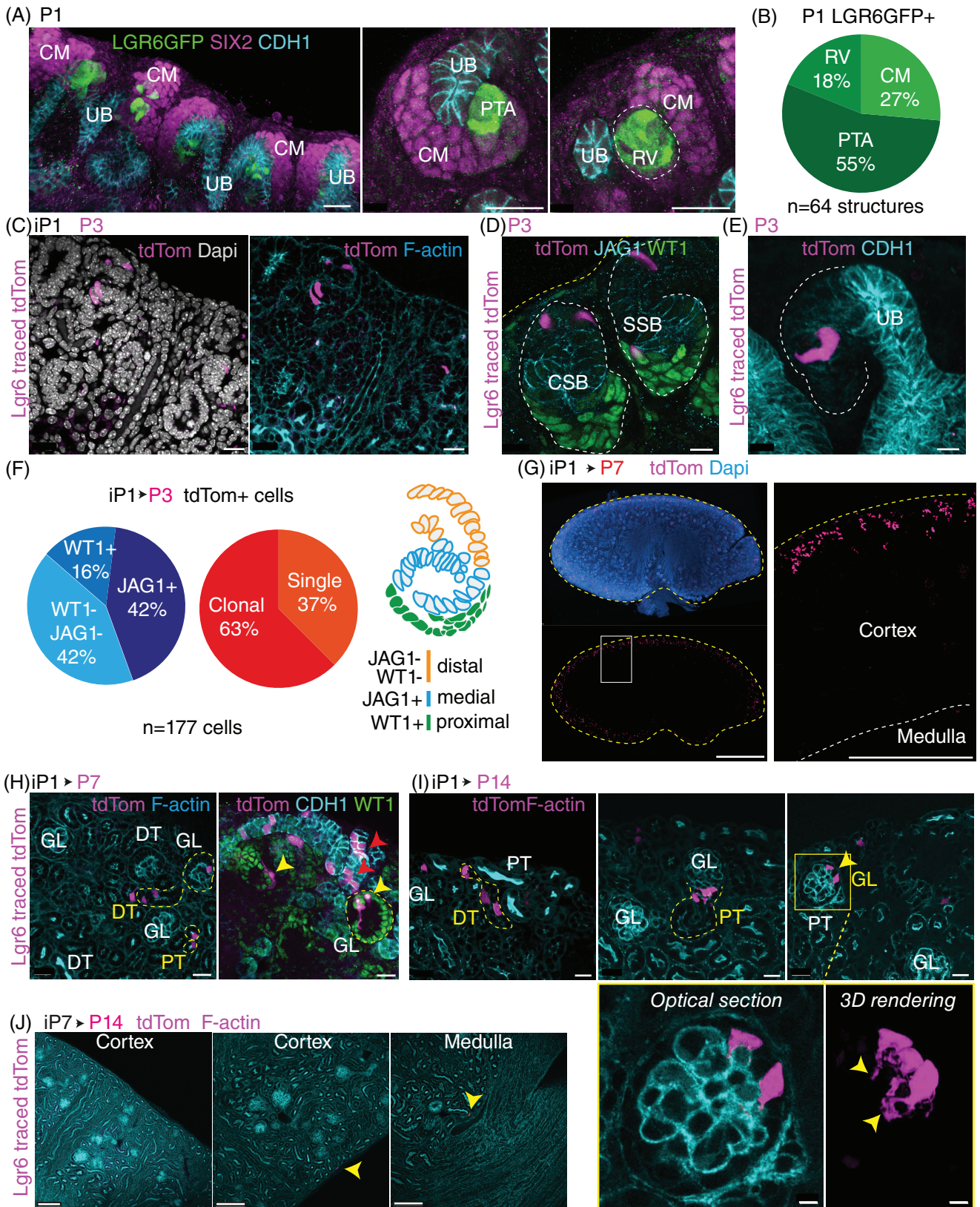


FIGURE 5 Legend on next page.

4 | EXPERIMENTAL PROCEDURES

4.1 | Mice and animal care

LGR6-EGFP-IRES-CreERT2 mice were kindly provided by Prof. Hans Clevers and described previously.¹³ LGR6-EGFP-IRES-CreERT2-ROSA26-tdTomato mice were obtained by crossing LGR6-EGFP-IRES-CreERT2 to ROSA26-tdTomato mice.²⁵ All animal experiments were approved by the animal experimentation committees of the Royal Dutch Academy of Science, the Hubrecht Institute and the Princes Máxima Center for Pediatric Oncology. IvD Maxima-Study protocol: PMC.60.3067.1805 CCD License: PMCAVD3990020173067.

4.2 | Immunohistochemistry vibratome sections

LGR6-EGFP-IRES-CreERT2 embryos were fixed overnight in 4% paraformaldehyde (PFA) at 4°C and embedded in 4% Agarose (Invitrogen), dissolved in mQ and sectioned using a vibratome (Thermo Scientific Microm, HM 650 V). Sections (100–200 µm) were washed three times in 0.5% Triton-X100 in PBS, permeabilized, and blocked with 5% donkey serum and 0.5% Triton-X100 in PBS0 for 1 hour at room temperature (RT). The primary antibodies goat anti-GFP (1:1000, GR287379-3, Abcam), rat anti-Ecadherin (1:600, DECMA-1, AbCam), rabbit anti-Six2 (1:400, 11 562-I AP, Protein Technologies), and goat anti-jagged (1:300, C-20; Santa Cruz) were incubated overnight in PBS0 + 5% donkey serum at 4°C. The sections were incubated with the secondary antibodies Alexa Fluor 488 anti-goat, Alexa Fluor 555 anti-rat, Alexa Fluor

647 anti-rabbit (all 1:250, Life Technologies) for 1 hour at room temperature in PBS0 + 5% donkey serum for 1 hour at RT. To visualize DNA, the sections were incubated with 2 µg/mL Dapi for 15 minutes at RT. Sections were mounted on slides and images captured on a Leica SPE, SP5, and SP8 confocal microscope.

4.3 | Large-scale single-cell resolution 3D imaging

Kidneys from LGR6-EGFP-IRES-CreERT2 embryos were isolated, kept on ice and fixed in 4% PFA (Sigma-Aldrich) for 2 hours at 4°C. LSR-3D imaging was performed as described previously.¹⁷ In short, kidneys were washed with PBT (PBS, 0.1% Tween) and incubated overnight with primary antibodies; goat anti-GFP (1:200, GR287379-3, Abcam), rabbit anti-Six2 (1:200, 11 562-I AP, Protein Technologies), and rat anti-Ecad (1:500, DECMA-1, AbCam). The next day, kidneys were washed with PBT and incubated overnight at 4°C with secondary antibodies and Alexa-fluor-555 Phalloidin (all from Thermo Fisher Scientific). Optical clearing was achieved by overnight incubation with FUnGI. Imaging was performed on a Zeiss LSM 880 using a ×25 oil immersion objective. Imaris imaging software was used for 3D rendering of images.

4.4 | Single cell segmentation and quantification

Image analysis was performed using Arivis Vision4D 3.0 equipped with the membrane based cell segmentation

FIGURE 5 In vivo lineage tracing and 3D imaging reveals contribution to nephrons by postnatal *Lgr6*⁺ cells. (A) Representative images of P1 LGR6-EGFP-IRES-CreERT2 vibratome sectioned kidneys stained with anti-SIX2 (magenta), anti-CDH1 (cyan) and anti-GFP (green). Scale bars 30 µm. (B) Pie chart representing the distribution and localization of LGR6-GFP⁺ cells at P1 per RV, PTA, and CM of 64 structures quantified in total. (C) Representative vibratome section of P3 LGR6-EGFP-IRES-CreERT2/ROSA26-tdTomato kidneys of pups injected with tamoxifen at P1 and stained with dapi (gray) and F-actin (cyan). TdTom⁺ cells in magenta. Scale bar 20 µm. (D) Representative P3 LGR6-EGFP-IRES-CreERT2/ROSA26-tdTomato kidneys of pups injected with tamoxifen at P1 and stained with anti-JAG1 (cyan) and anti-WT1 (green). TdTom⁺ cells in magenta. Scale bar 10 µm. (E) Representative P3 LGR6-EGFP-IRES-CreERT2/ROSA26-tdTomato kidneys of pups injected with tamoxifen at P1 and stained with anti-CDH1 (cyan). TdTom⁺ cells in magenta. Scale bar 10 µm. (F) Pie charts representing marker positivity (blue) and distribution (red) of tdTom⁺ cells at P3 (n = 177 cells). (G) P7 LGR6-EGFP-IRES-CreERT2/ROSA26-tdTomato kidneys of pups injected with tamoxifen at P1 and stained with Dapi (blue). TdTom⁺ cells in magenta. Cortex and medulla indicated by dashed lines. Right panel shows magnification of cortex region indicated in left panel. Scale bar 1 mm. (H) P7 LGR6-EGFP-IRES-CreERT2/ROSA26-tdTomato kidneys of pups injected at P1/P2/P3 with tamoxifen and stained with F-actin (cyan), or with anti-WT1 (green) and anti-CDH1 (cyan). TdTom⁺ cells in magenta. Red arrowheads indicate TdTom⁺ CDH1⁺ tubular cells, yellow arrowheads indicate TdTom⁺ WT1⁺ cells. Scale bars 20 µm. (I) Representative cortex regions of P14 LGR6-EGFP-IRES-CreERT2/ROSA26-tdTomato kidneys of pups injected with tamoxifen at P1/P2/P3 and stained with F-actin (cyan). TdTom⁺ cells in magenta. Yellow dashed lines represent DT and PT. Yellow inset is a magnification of a GL. Scale bars 20 µm. Yellow arrows indicate 3D rendered podocyte like cells. Scale bars 5 µm for magnified panels GL inset and 3D rendering. (J) Representative P14 LGR6-EGFP-IRES-CreERT2/ROSA26-tdTomato kidneys of pups injected with tamoxifen at P7 and stained with F-actin (cyan). TdTom⁺ cells in magenta indicated by yellow arrowheads

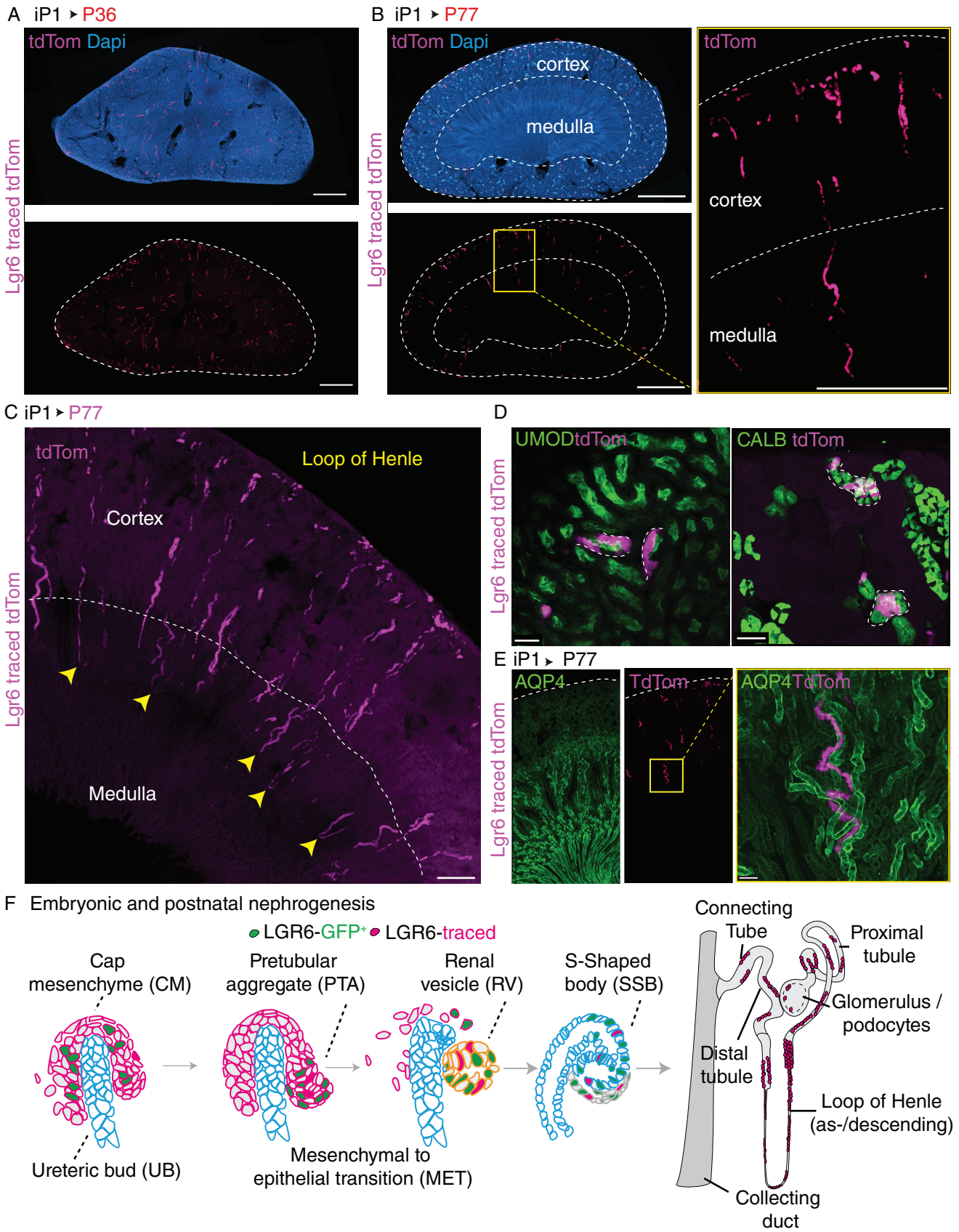


FIGURE 6 Legend on next page.

method as described previously.²⁶ For LGR6-GFP⁺ quantification we analyzed regions of interest (ROI) containing CM and different stages of nephron development based on tissue morphology as seen by F-actin staining. As a preprocess for segmentation, the F-actin channel was enhanced using the Membrane Enhancement filter. Subsequently, the Membrane based Segmenter was used to segment this enhanced membrane channel into individual cells. These were stored as objects that can then be filtered on size and Lgr6 intensity to obtain Lgr6 positive cells. The resulting object selection was manually refined to remove false positives coming from noise of the anti-GFP antibody staining. The exported mean intensities of SIX2 and CDH1 of the LGR6⁺ selections were normalized to the highest mean intensity cell in the analyzed ROI and plotted per developmental compartment.

4.5 | Ex vivo embryonic kidney culture

Embryos from timed pregnancies of approximately 11 days of gestation were harvested using a dissecting microscope as described previously.²⁷ The embryos were placed in a PBS containing Petri-dish. After removal of the head, the posterior piece was placed with the dorsal side down. The abdominal wall was opened, and intra-abdominal contents were removed to expose the mesonephros retroperitoneum. The retroperitoneal plate mesonephros was removed and the kidneys were isolated from it. The developing kidneys were placed on a transwell filter (Greiner Bio-One) within a 24-well tissue culture dish containing 600 μ L medium Dulbecco's modified Eagle medium (DMEM, Gibco, Invitrogen) supplemented with fetal calf serum (10% FCS, Sigma) and 1% Streptomycin/penicillin (100 μ g/mL Streptomycin; 100 μ /mL Penicillin, Invitrogen) to culture them on a liquid air interface. The culture was maintained for 7 days in a fully humidified 37°C incubator with 5% CO₂, by replacing the medium every second day. Images were taken using an Evos FL microscope. Time lapses were obtained using a Leica AF7000 widefield

fluorescence microscope. After 1 week of culture, the kidneys were removed from the filter and fixed for 30 minutes in Periodate-lysine-paraformaldehyde fixative (pH = 7.4) at RT. The kidneys were washed three times in 0.5% Triton-X 100 in PBS0. Permeabilization and blocking was obtained by incubating the sections in 5% donkey serum and 0.5% Triton-X 100 in PBS0 for 30 minutes at RT. Primary antibodies were incubated for 1 hour and 30 minutes in PBS0 + 5% donkey serum at RT. The sections were incubated with the secondary antibodies Alexa Fluor 488 donkey anti-rat, Alexa Fluor 647 donkey anti-rabbit (both 1:250, Life Technologies) for 45 minutes at RT in PBS0 + 5% donkey serum. To visualize the DNA, the sections were incubated with 2 μ g/mL Dapi for 10 minutes at RT. Images were captured on a Leica SPE/SP8 confocal microscope.

4.6 | Ex vivo and in vivo lineage tracing

For ex vivo lineage tracing, after embryo isolation, the embryonic kidneys were incubated in 0.5-1.0 μ M 4-hydroxy-tamoxifen (4-OHT) for 1 hour. Time lapse imaging over multiple days were obtained using a Leica AF7000 widefield fluorescence microscope and still images were obtained using an Evos FL microscope. For in vivo lineage tracing, postnatal pups were injected with Tamoxifen (100 μ L/10 mg/mL) daily and at P1, P2, and P3.

4.7 | Fluorescence activated cell sorting and single-cell RNA-sequencing

4.7.1 | Cell sorting

LGR6-EGFP-IRES-CreERT2 kidneys isolated at E11.5 were disaggregated into single cells by collagenase treatment. For characterization by single cell RNA seq, cells were sorted into 384 well plates using the BD fluorescence activated cell sorting (FACS) Aria II. LGR6-EGFP-

FIGURE 6 In vivo lineage tracing and 3D imaging reveals contribution to nephrons by postnatal Lgr6⁺ cells. (A,B) Representative P36 (A) and P77 (B) LGR6-EGFP-IRES-CreERT2/ROSA26-tdTomato kidneys of pups injected with tamoxifen at P1 and stained with dapi (blue). TdTom⁺ cells in magenta. Cortex and medulla indicated by dashed lines. Scale bar 1 mm. (C) Representative area of a P77 LGR6-EGFP-IRES-CreERT2/ROSA26-tdTomato kidney of pups injected with tamoxifen at P1/P2/P3. TdTom⁺ clones in magenta depicting ribbons of loop of Henle (yellow arrows). Scale bar 300 μ m. (D) Representative P77 LGR6-EGFP-IRES-CreERT2/ROSA26-tdTomato kidneys of pups injected with tamoxifen at P1/P2/P3 and stained with anti-UMOD or anti-CALBINDIN in green. TdTom⁺ clones in magenta. Dashed lines outline the tubules. Scale bars 50 μ m. (E) P77 LGR6-EGFP-IRES-CreERT2/ROSA26-tdTomato kidneys of pups injected with tamoxifen at P1 and stained with anti-Aqp4 (green). Right panel depicts magnification of area indicated in left panel. TdTom⁺ clones in magenta. Scale bar 50 μ m. (F) Graphic representation of embryonic and postnatal LGR6-GFP expression (green cells) and lineage traced cells (red cells) during nephron development

IRES-CreERT2/ROSA26-tdTomato kidneys isolated at E11.5 were induced in 4-OHT (0.5 mM) for 1 hour and after washing carefully, cultured for 7 days as described. After 1 week of culture, the kidneys were removed from the filter and washed in DMEM (10% FCS, 1% P/S) and disaggregated into single cells by collagenase treatment. For characterization by single cell RNA seq, tdTomato⁺ cells were sorted in 384 well plates on the BD FACS Aria II.

4.7.2 | Sample preparation

Samples were prepared according to the SORT-seq method.²⁸ Viable single cells were sorted based on forward/side scatter properties and DAPI staining using FACS (into 384-well plates [Biorad] containing 10 µl mineral oil [Sigma]) and 50 nl of RT primers. Samples were subsequently processed into Illumina sequencing libraries as described.²⁸ Libraries were sequenced paired end at 75 bp read length using the Illumina NextSeq500 sequencer.

4.7.3 | Data processing

Sequencing data was processed using the Sharq pipeline (<https://doi.org/10.1101/250811>). We performed the mapping using STAR version 2.6.1 on the Genome Reference Consortium Mouse Build 38 and the transcripts present in the respective constructs. Read assignment was with feature Counts version 1.5.2 using a gene annotation based on GENCODE version M14. scRNAseq is available and accessible under ID GSE16479 <https://www.ncbi.nlm.nih.gov/geo/query/acc.cgi?acc=GSE164795>

4.7.4 | Analysis

Transcripts mapping to the mitochondrial genome and external RNA controls (ERCCs) were removed. Cells with fewer than 1000 unique transcripts were also removed. After gene and cell filtering, unique transcript counts were normalized to 10 000. Analysis was performed using the Seurat R package version 2.3.4.²⁹ To avoid clustering of cells based on transgenes' expression, cell cycle phase profiles, dissociation stress, or activity, the following genes were removed from the variant genes list used for clustering estimation, but included back for further analysis: the non-mouse genes introduced in the strains (GFP, TdTom, NeoR, and Cre), the cell-cycle associated genes, as defined in Ref. 30, heat shock protein genes, as defined by GO Term GO:0006986—response to unfolded

protein, as well as ribosomal protein genes, based on the GO term GO:0022626—cytosolic ribosome. For the E11.5 GFP dataset, the first 15 principal components (PCs) were used for graph-based clustering; for the ex vivo *TdTom* dataset the first 21 PCs were used. Differential expression analysis was performed using the Wilcoxon test with 1.8-fold expression difference cut-off and a statistical significance cut-off of 0.05 (Bonferroni multiple testing corrected). Human to mouse orthology mapping was done using biomaRt³¹ and selection of the top 20 markers of different cell clusters was performed as described before.³² Lineage scoring was performed using Seurat's AddModuleScore function.²⁹

ACKNOWLEDGMENTS

We like to thank the Princess Máxima Center Single Cell Genomics, Princess Máxima Imaging Center and the Hubrecht Institute single cell sequencing and FACS facilities. We thank Utrecht Sequencing Facility for providing sequencing service and data. Utrecht Sequencing Facility is subsidized by the University Medical Center Utrecht, Hubrecht Institute, Utrecht University and The Netherlands X-omics Initiative (NWO project 184.034.019). This work was financially supported by the Princess Máxima Center for Pediatric Oncology. FLB was supported by the Dutch Cancer Society (KWF) fellowship (ID# 6660). ACR was awarded the St. Baldrick's Robert J. Arceci International Innovation award and is supported by an ERC-starting grant 2019, project 804412. EJW is supported by Cancer GenomiCs (CGC). TM, PL and FH were supported by European Research Council (ERC) Advanced Grant [671174]; JvR was supported by the European Research Council Grant CANCER-RECURRENCE 648804, the CancerGenomics.nl (Netherlands Organization for Scientific Research) program and the Doctor Josef Steiner Foundation.

CONFLICT OF INTEREST

The authors declare no conflicts of interest.

AUTHOR CONTRIBUTIONS

Ravian van Ineveld: Conceptualization; data curation; formal analysis; investigation; writing-review & editing. **Thanasis Margaritis:** Conceptualization; data curation; formal analysis; investigation; methodology; resources; software; visualization; writing-review & editing. **Berend Kooiman:** Data curation; formal analysis; investigation; visualization. **Femke Groenveld:** Data curation; formal analysis; investigation; methodology; visualization. **Rijndert Ariese:** Formal analysis; methodology. **Philip Lijnzaad:** Data curation; investigation; methodology; resources; visualization. **Jeroen Korving:** Methodology. **Hannah Johnson:** Methodology; resources; supervision.

Ellen Wehrens: Writing-original draft; writing-review & editing. **Frank Holstege:** Conceptualization; investigation; supervision. **Jacco Rheenen:** Funding acquisition; project administration; supervision. **Jarno Drost:** Conceptualization; supervision. **Anne Rios:** Funding acquisition; supervision; writing-review & editing. **Frank Bos:** Conceptualization; data curation; formal analysis; funding acquisition; investigation; methodology; project administration; resources; software; supervision; validation; visualization; writing-original draft; writing-review & editing.

DATA AVAILABILITY STATEMENT

The scRNA-seq has been deposited in the Gene Expression Omnibus database, accessible under ID GSE164795 <https://www.ncbi.nlm.nih.gov/geo/query/acc.cgi?acc=GSE164795>

ORCID

Thanasis Margaritis  <https://orcid.org/0000-0003-4040-2015>

Frank L. Bos  <https://orcid.org/0000-0003-3811-8330>

REFERENCES

- Kopan R, Chen S, Little M. Nephron progenitor cells. Shifting the balance of self-renewal and differentiation. *Current Topics in Developmental Biology*. Vol 107. Cambridge, MA: Academic Press Inc.; 2014:293-331. <https://doi.org/10.1016/B978-0-12-416022-4.00011-1>.
- Karner CM, Das A, Ma Z, et al. Canonical Wnt9b signaling balances progenitor cell expansion and differentiation during kidney development. *Development*. 2011;138(7):1247-1257. <https://doi.org/10.1242/dev.057646>.
- Kobayashi A, Valerius MT, Mugford JW, et al. Six2 defines and regulates a multipotent self-renewing nephron progenitor population throughout mammalian kidney development. *Cell Stem Cell*. 2008;3(2):169-181. <https://doi.org/10.1016/j.stem.2008.05.020>.
- Carroll TJ, Das A. Defining the signals that constitute the nephron progenitor niche. *J Am Soc Nephrol*. 2013;24(6):873-876. <https://doi.org/10.1681/ASN.2012090931>.
- Boyle SC, Kim M, Valerius MT, McMahon AP, Kopan R. Notch pathway activation can replace the requirement for Wnt4 and wnt9b in mesenchymal-to-epithelial transition of nephron stem cells. *Development*. 2011;138(19):4245-4254. <https://doi.org/10.1242/dev.070433>.
- Stark K, Vainio S, Vassileva G, McMahon AP. Epithelial transformation of metanephric mesenchyme in the developing kidney regulated by Wnt-4. *Nature*. 1994;372(6507):679-683. <https://doi.org/10.1038/372679a0>.
- Lindström NO, De Sena Brandine G, Tran T, et al. Progressive recruitment of Mesenchymal progenitors reveals a time-dependent process of cell fate Acquisition in Mouse and Human Nephrogenesis. *Dev Cell*. 2018;45(5):651-660. <https://doi.org/10.1016/j.devcel.2018.05.010>.
- Boyle S, Misfeldt A, Chandler KJ, et al. Fate mapping using Cited1-CreERT2 mice demonstrates that the cap mesenchyme contains self-renewing progenitor cells and gives rise exclusively to nephronic epithelia. *Dev Biol*. 2008;313(1):234-245. <https://doi.org/10.1016/j.ydbio.2007.10.014>.
- Barker N, Tan S, Clevers H. Lgr proteins in epithelial stem cell biology. *Development*. 2013;140(12):2484-2494. <https://doi.org/10.1242/dev.083113>.
- Barker N, Rookmaaker MB, Kujala P, et al. Lgr5+ve stem/progenitor cells contribute to nephron formation during kidney development. *Cell Rep*. 2012;2(3):540-552. <https://doi.org/10.1016/j.celrep.2012.08.018>.
- Kinzel B, Pikiólek M, Orsini V, et al. Functional roles of Lgr4 and Lgr5 in embryonic gut, kidney and skin development in mice. *Dev Biol*. 2014;390(2):181-190. <https://doi.org/10.1016/j.ydbio.2014.03.009>.
- Mohri Y, Oyama K, Akamatsu A, Kato S, Nishimori K. Lgr4-deficient mice showed premature differentiation of ureteric bud with reduced expression of Wnt effector Lef1 and Gata3. *Dev Dyn*. 2011;240(6):1626-1634. <https://doi.org/10.1002/dvdy.22651>.
- Snippert HJ, Haegerbarth A, Kasper M, et al. Lgr6 marks stem cells in the hair follicle that generate all cell lineages of the skin. *Science (80)*. 2010;327(5971):1385-1389. <https://doi.org/10.1126/science.1184733>.
- Blaas L, Pucci F, Messal HA, et al. Lgr6 labels a rare population of mammary gland progenitor cells that are able to originate luminal mammary tumours. *Nat Cell Biol*. 2016;18(12):1346-1356. <https://doi.org/10.1038/ncb3434>.
- Lehoczy JA, Tabin CJ. Lgr6 marks nail stem cells and is required for digit tip regeneration. *Proc Natl Acad Sci U S A*. 2015;112(43):13249-13254. <https://doi.org/10.1073/pnas.1518874112>.
- Chung E, Deacon P, Marable S, Shin J, Park JS. Notch signaling promotes nephrogenesis by downregulating Six2. *Development*. 2016;143(21):3907-3913. <https://doi.org/10.1242/dev.143503>.
- Rios AC, Capaldo BD, Vaillant F, et al. Intracloonal plasticity in mammary tumors revealed through large-scale single-cell resolution 3D imaging. *Cancer Cell*. 2019;35(4):618-632. <https://doi.org/10.1016/j.ccell.2019.02.010>.
- Stewart BJ, Ferdinand JR, Young MD, et al. Spatiotemporal immune zonation of the human kidney. *Science (80)*. 2019;365(6460):1461-1466. <https://doi.org/10.1126/science.aat5031>.
- Tögel F, Valerius MT, Freedman BS, Latrino R, Grinstein M, Bonventre JV. Repair after nephron ablation reveals limitations of neonatal nephrogenesis. *JCI Insight*. 2017;2(2). <https://doi.org/10.1172/jci.insight.88848>.
- Hartman HA, Lai HL, Patterson LT. Cessation of renal morphogenesis in mice. *Dev Biol*. 2007;310(2):379-387. <https://doi.org/10.1016/j.ydbio.2007.08.021>.
- Kumaran GK, Hanukoglu I. Identification and classification of epithelial cells in nephron segments by Actin cytoskeleton patterns. *FEBS J*. 2020;287(6):1176-1194. <https://doi.org/10.1111/febs.15088>.
- Lawlor KT, Zappia L, Lefevre J, et al. Nephron progenitor commitment is a stochastic process influenced by cell migration. *Elife*. 2019;8. <https://doi.org/10.7554/eLife.41156>.

23. Pode-Shakked N, Pleniceanu O, Gershon R, et al. Dissecting stages of human kidney development and tumorigenesis with surface markers affords simple prospective purification of nephron stem cells. *Sci Rep*. 2016;6. <https://doi.org/10.1038/srep23562>.
24. Metsuyanin S, Harari-Steinberg O, Buzhor E, et al. Expression of stem cell markers in the human fetal kidney. *PLoS One*. 2009;4(8). <https://doi.org/10.1371/journal.pone.0006709>.
25. Madisen L, Zwingman TA, Sunkin SM, et al. A robust and high-throughput Cre reporting and characterization system for the whole mouse brain. *Nat Neurosci*. 2010;13(1):133-140. <https://doi.org/10.1038/nn.2467>.
26. Mosaliganti KR, Noche RR, Xiong F, Swinburne IA, Megason SG. ACME: automated cell morphology extractor for comprehensive reconstruction of cell membranes. *PLoS Comput Biol*. 2012;8(12). <https://doi.org/10.1371/journal.pcbi.1002780>.
27. Riccio PN, Michos O. Dissecting and culturing and imaging the mouse urogenital system. *Methods Mol Biol*. 2012;886:3-11. https://doi.org/10.1007/978-1-61779-851-1_1.
28. Muraro MJ, Dharmadhikari G, Grün D, et al. A single-cell Transcriptome atlas of the human pancreas. *Cell Syst*. 2016;3(4):385-394.e3. <https://doi.org/10.1016/j.cels.2016.09.002>.
29. Butler A, Hoffman P, Smibert P, Papalexi E, Satija R. Integrating single-cell transcriptomic data across different conditions, technologies, and species. *Nat Biotechnol*. 2018;36(5):411-420. <https://doi.org/10.1038/nbt.4096>.
30. Scialdone A, Natarajan KN, Saraiva LR, et al. Computational assignment of cell-cycle stage from single-cell transcriptome data. *Methods*. 2015;85:54-61. <https://doi.org/10.1016/j.ymeth.2015.06.021>.
31. Durinck S, Spellman PT, Birney E, Huber W. Mapping identifiers for the integration of genomic datasets with the R/ bioconductor package biomaRt. *Nat Protoc*. 2009;4(8):1184-1191. <https://doi.org/10.1038/nprot.2009.97>.
32. Hanemaaijer ES, Margaritis T, Sanders K, et al. Single-cell atlas of developing murine adrenal gland reveals relation of Schwann cell precursor signature to neuroblastoma phenotype. *Proc Natl Acad Sci U S A*. 2021;118(5). <https://doi.org/10.1073/pnas.2022350118>.

SUPPORTING INFORMATION

Additional supporting information may be found online in the Supporting Information section at the end of this article.

How to cite this article: van Ineveld RL, Margaritis T, Kooiman BAP, et al. LGR6 marks nephron progenitor cells. *Developmental Dynamics*. 2021;250(11):1568–1583. <https://doi.org/10.1002/dvdy.346>